Dielectric Relaxation in Liquid Crystalline/Isotropic Block Copolymers: Effect of Nanoscale Confinement on the Segmental Dynamics

Sergei Zhukov,[†] Steffen Geppert,[‡] Bernd Stühn,*[,†] Rosina Staneva,[†] Rouja Ivanova,[†] and Wolfram Gronski[‡]

Technical Physics II/Polymer Physics, Ilmenau Technical University, PF 100565, 98684 Ilmenau, Germany; and Institute for Macromolecular Chemistry, Albert-Ludwigs-University, 79104 Freiburg, Germany.

Received April 1, 2002

ABSTRACT: We have synthesized a series of liquid crystalline/isotropic block copolymers with narrow molecular weight distribution and with well-defined chemical structure. Block volume fractions were varied systematically. The domain structure of these compounds was determined by means of small-angle X-ray scattering. Spherical, cylindrical, and lamellar morphologies were observed with the liquid crystalline (LC) block in the matrix or in the domain, respectively. The polymers are strongly segregated, and no order-to-disorder transition is found up to 170 °C. DSC and polarized microscopy data reveal that the mesomorphic behavior of LC blocks is only slightly influenced by copolymer composition and is basically characterized by the sequence g/∼35 °C/n/∼120 °C/i. The rotational dynamics over a broad temperature and frequency range was studied using dielectric spectroscopy. The LC block reveals two cooperative modes assigned to the segmental relaxation (α process) and to the side chain rotation as a whole (δ process). A confinement effect is visible in the shift of both relaxation times to lower values for domain sizes less than 20 nm. The effect is stronger for 2D than for 1D confinement geometry. It is small compared to similar effects found for free-standing thin polymer films. For copolymers with alternate lamellae or LC cylindrical microdomains, a Maxwell−Wagner polarization was observed in addition to the α and δ processes.

1. Introduction

The mechanism involved in the glass transition is not yet fully understood at the current time. Glass transitions in finite systems confined to nanopores[1−12] and ultrathin polymer films[13−23] have recently attracted much attention, because such systems can be regarded as model compounds for studying the length scale of the glass transition. In such a system, deviations from bulk (unconfined) properties are expected to appear if the system size is comparable to the characteristic length scale of the glass transition. It was documented in several studies that the α process, which reflects the dynamic glass transition, speeds up and the relaxation time distribution broadens for the confined state.[2−4,6−9,21−23] However, this finding is not confirmed by all studies,[1,5,12,20] and further experimental work is necessary to explain this phenomenon.

Block copolymers are particularly interesting compounds in this respect. They allow studying the dynamics of molecules in restricted geometry created by microphase separation. The common types of domain forms are spheres, cylinders, and lamellae representing the cases of three- (3D), two- (2D), and one-dimensional (1D) confinement, respectively. Type and dimension of the mesostructure can be controlled at the level of synthesis. This idea has been exploited for the case of isotropic block copolymers for different morphologies.[24−26] In particular, the use of segmental and normal modes of dielectric spectroscopy enabled the investigation of relaxation on different length scales. The effect of the microphase separation transition on the segmental dynamics is clearly seen in the relaxation time and the width of the normal mode.[27]

The main topic of this study is the investigation of the molecular dynamics of a series of liquid crystalline/isotropic (LC/I) block copolymers with well-defined chemical structure by means of dielectric spectroscopy. Block volume fractions are varied in a wide range thus allowing us to obtain copolymers with different types of nanoscale confinement (1D, 2D, and 3D). The polymers investigated consist of two different blocks: a LC (liquid crystalline) block and an isotropic PS (polystyrene) block. The LC block has the structure of a liquid crystalline side chain polymer. A rigid cyanobiphenyl mesogen fragment is connected to the main butadiene chain via a flexible alkyl spacer. Its strong dipole moment is the main source of dielectric relaxation in this material. We have synthesized and studied 10 compositions (including the LC homopolymer).

The mesomorphic behavior of the copolymers was determined via DSC analysis. To relate the results from the dynamic experiment to the spatial confinement, domain sizes and forms have to be known as well as their variation with temperature. This information was obtained from detailed structure analysis using small-angle X-ray scattering (SAXS).

2. Experimental Section

Synthesis of the LC/I Block Copolymers. A series of liquid crystalline nematic side chain/isotropic diblock copolymers with systematically varied block volume ratios were synthesized through a modified three-step technique developed earlier by Gronski et al.[28] The isotropic block of the copolymers is polystyrene, and the liquid crystalline block consists of cyanobiphenyl mesogens coupled to poly(1,2-butadiene) through valeric acid spacers (Figure 1). The polymers are denoted as PSLC *x*/*y*, where *x* is the content of the PS block in volume

* To whom correspondence should be addressed.
[†] Ilmenau Technical University.
[‡] Albert-Ludwigs-University.

10.1021/ma020509+ CCC: $22.00
Published on Web 09/28/2002

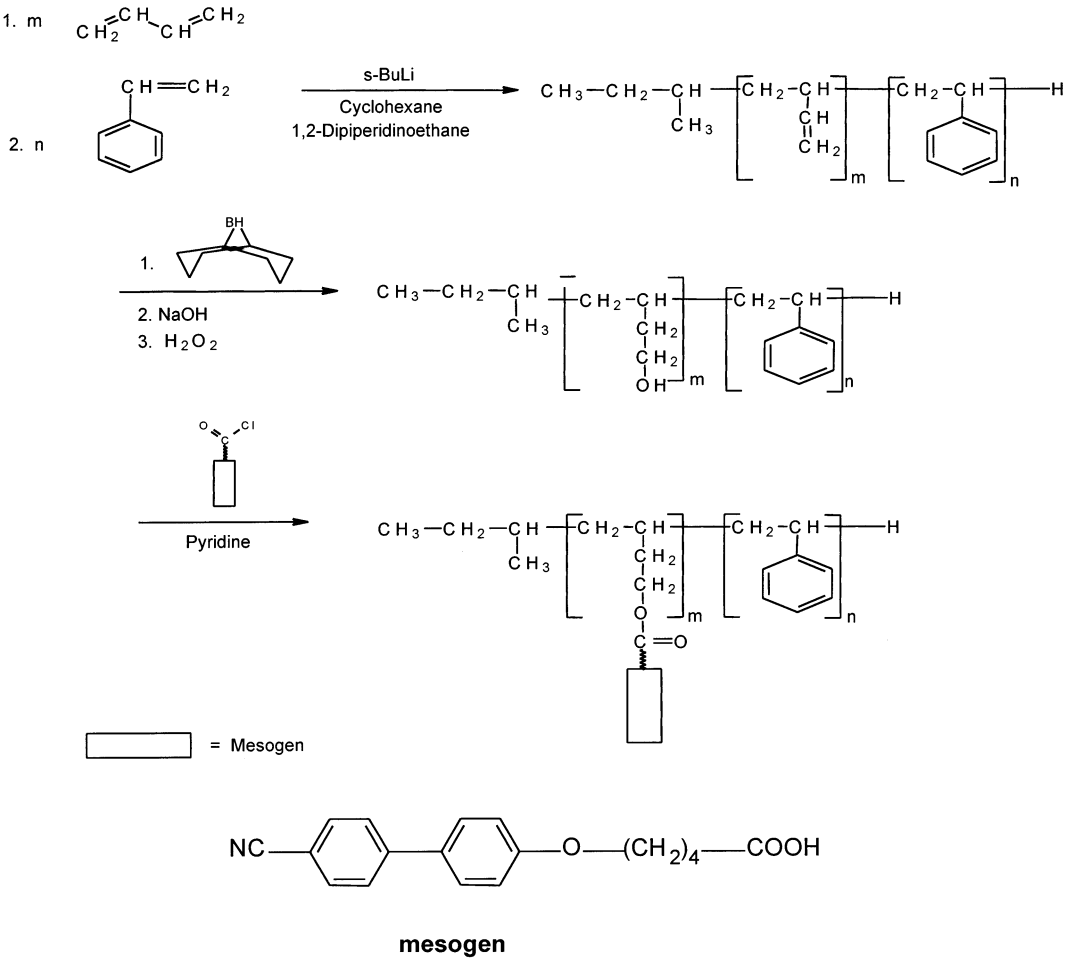

Figure 1. Route of synthesis.

percent and *y* is the content of the LC block. In the first step of synthesis, polystyrene-*b*-poly(1,2-butadiene) precursor block copolymers (PSPB) with strictly defined molecular weight and block volume ratios were synthesized through living anionic polymerization. In the second step, the vinyl 1,2-double bonds of the PB block of the precursor copolymers were converted into OH groups (the obtained polymers denoted as PSOH) through hydroboration with 9-BBN. The mesogen unit was prepared by coupling of the cyanobiphenyl mesogen to a valeric acid spacer by etherification. In the third step, the mesogen unit was inserted in the PSOH block copolymers through esterification of the OH groups with the activated mesogenic groups. The excess of unbound mesogen units, which can severely disturb the dielectric experiments, was removed from the product by a novel combination of dialysis column chromatography and continuos extraction in various solvents depending on the solubility of the corresponding block copolymers. After purification, the LC/I block copolymers did not show any low molecular weight impurities (proved by SEC). Modification of the synthesizing technique was necessary because of the difficulties posed by its earlier variant in attaining polymers with strictly defined molecular weight, termination of the polymerization without side-reactions, and purification of the solvent under the given conditions. A particular problem was encountered for block copolymers with extremely asymmetric composition concerning their solubility and solubility changes during the second and third step of synthesis. This problem was solved through an improvement of the method of synthesis, modification of the apparatus, novel terminating method, modified control of the solvent polarity during the reaction, and use of various solvent combinations.

The LC/I diblock copolymers were characterized using SEC for determination of molecular weight and ^{1}H NMR for determination of the composition of the PSPB block copolymers (data shown in Table 1). FTIR and ^{1}H NMR proved that both polymer analogous reactions (step two and step three) proceed with 100% conversion and without side reactions. The molecular weight polydispersity of the precursor block copolymers is very narrow ($M_w/M_n \leq 1.1$) and essentially does not change during the two conversion reactions.

Small-Angle X-ray Scattering. SAXS measurements were performed using a Kratky compact small-angle system (PAAR, Graz, Austria) equipped with a scintillation counter operating in a step-scanning mode. Cu Kα radiation of wavelength 1.54 Å was provided by a sealed X-ray tube and an X-ray generator (Kristalloflex 710H, Siemens Germany). A Ni filter was used to suppress the contribution from K_β radiation. The sample-to-detector distance was 200 mm. The camera volume was kept under vacuum during the measurements to reduce background scattering from air. A temperature-controllable sample holder with filament and a Eurotherm 2404 controller provided temperature stabilization at 25−150 °C with a precision of ±0.1 °C. Samples of the block copolymers representing solid homogeneous bars with 2 mm thickness were prepared in the following way. The block copolymer powder was placed in a steel tool and pressed, then heated to 150 °C to melt, and annealed under vacuum. The temperature was chosen to be above the T_g of the PS block (∼100 °C) and above the T_g (∼30 °C) and the T_{ni} (112−123 °C) of the LC block. SAXS spectra were measured in heating and cooling cycles in steps of 10 deg. Following each temperature change the sample was equilibrated for 30 min. Subtraction of the background scattering, normalization, and desmearing of the recorded slit-smeared spectra were done using standard procedures.[29] The normalization of the scattering intensity to the incoming X-ray flux measured with the moving slit device (PAAR, Graz, Austria) results in the absolute intensity in units of the Thompson cross section as a function of the scattering vector

Table 1. Characteristics of the Synthesized Precursor and LC/I Diblock Copolymers

	precursor PSPB polymers[a]				PSLC polymers[b]				
polymer	MW	PS (wt %)	PB (wt %)	M_w/M_n	MW	PS (wt %)	LC (wt %)	PS (vol %)	LC (vol %)
PSLC 7/93	15 600	27.9	72.1	1.06	77 000	5.7	94.3	6.8	93.2
PSLC 14/86	13 200	45.5	54.5	1.06	53 700	11.5	88.5	13.5	86.5
PSLC 19/81	30 500	55.6	44.4	1.10	104 300	16	84	19	81
PSLC 30/70	36 500	69.3	30.7	1.08	98 700	26	74	30	70
PSLC 39/61	23 600	77.3	22.7	1.10	55 000	34.5	65.5	38.8	61.2
PSLC 59/41	23 500	88.5	11.5	1.03	38 300	54.5	45.6	58.9	41.1
PSLC 77/23	48 800	94.7	5.3	1.03	62 800	73.4	26.6	76.8	23.2
PSLC 85/15	71 200	96.8	3.2	1.05	86 500	82.5	17.5	85	15
PSLC 97/3	122 000	99.5	0.5	1.05	125 000	96.9	3.1	97.4	2.6

[a] Experimentally measured data. [b] Data for the molecular weight and wt % were calculated stoichiometrically on the basis of 100% conversion. Data for the vol % were calculated using the density of the PS block (1.04 g/cm^3) and of the LC block (1.25 g/cm^3).

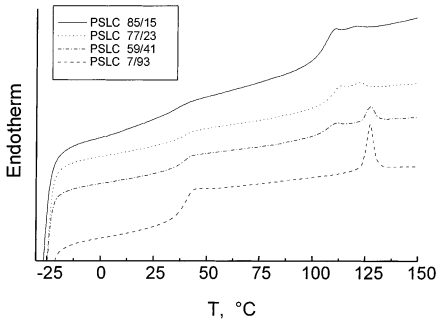

Figure 2. DSC scans for selected PSLC copolymers recorded at a heating rate of 10 deg/min.

Table 2. Transition Temperatures of the Investigated Copolymers

	T_g (°C)		T_{ni} (°C)	
polymer	PS	LC	DSC	polarized microscope
PSLC 0/100		33.5	112.1	
PSLC 7/93		32.0	116.1	121.5
PSLC 14/86		35.4	116.9	
PSLC 19/81		31.2	110.3	
PSLC 30/70	104.3	33.3	117.1	
PSLC 39/61	102.2	35.1	117.9	
PSLC 59/41	104.0	35.6	121	121−123
PSLC 77/23	106.1	35.7	116	113−118
PSLC 85/15	106.7		115	113−118
PSLC 97/3	108.9			

$s = 2/\lambda(\sin\theta)$ (2θ: scattering angle). The desmearing corrects for the slitlike cross section of the X-ray beam and results in the so-called pinhole scattering profile.

Dielectric Spectroscopy (DS). Dielectric experiments in the wide frequency range $10^{-2}-10^{8}$ Hz were carried out by measuring the complex impedance with two different setups. In the range $10^{-2}-10^{6}$ Hz, we used the Solartron-Schlumberger frequency response analyzer SI1260 equipped with a Chelsea dielectric interface. In the range $10^{6}-10^{8}$ Hz, a rf impedance analyzer (HP 4191A) was employed. The sample capacitor consisted of two gold-coated stainless steel electrodes. It was filled with the polymer at 150 °C. The sample thickness was 0.05−0.1 mm. Sample temperature in the range 20−160 °C was controlled in a nitrogen gas jet (Quattro, Novocontrol GmbH) with stability better than 0.05 °C. Dielectric data were collected at fixed temperature in heating and cooling runs with temperature steps of 2−3 deg, allowing for sample equilibration after each temperature change.

3. Experimental Results and Discussion

3.1. Mesophase and Microdomain Structures. At all experimentally accessible temperatures (up to 170 °C), the block copolymers exist in the microphase separated state. We therefore expect to find two glass transitions related to both types of domains of the diblock copolymer. In addition to that, the nematic/isotropic transition (T_{ni}) of the LC block was determined using DSC and polarized microscopy. The thermal behavior for the selected compounds is illustrated in Figure 2. Both T_g's of the PS and the LC block are well distinguished in all thermograms except for those with the lowest PS or LC content, respectively. The transition temperature T_{ni} of the different copolymers is well resolved, except for PSLC 97/3. It lies in the interval 115−121 °C (Figure 2). The values of the T_g and the T_{ni} of the LC/I block copolymers are summarized in Table 2. On the basis of these data, it is concluded that nematic order exists inside the LC microdomains of the mesostructure at temperatures below the T_{ni} of the LC block. Only for the block copolymer with the lowest LC content PSLC 97/3 was it impossible to observe the formation of a nematic phase.

The domain structure of the liquid crystalline/isotropic block copolymers was determined from the analysis of their SAXS diffraction patterns. Details of this investigation are presented elsewhere.[29] Here we will only briefly discuss the temperature dependence of the microdomain structure and its characteristic length scales since these issues are of primary interest for the present investigation. All recorded scattering profiles show a well-defined, intense, and narrow first diffraction peak. In addition to that, several higher order diffraction peaks (second up to the sixth order) show up. These features of the scattering profiles are evidence for the microphase separated domain structure of the block copolymers. They thus confirm the result from the DSC data. Two glass transitions were observed in DSC scans, which is the case of well microphase segregated block copolymer systems with narrow interface between the two blocks. All these characteristics are indications that the block copolymers are strongly segregated.[30]

The only exception is the block copolymer with the lowest LC volume fraction, PSLC 97/3. Its diffraction pattern displays only one broad peak of low intensity. It does not vary with temperature as would be expected for a disordered diblock copolymer. Also, its DSC thermogram reveals only the glass transition of the PS block, lacking both the glass transition and the nematic/isotropic transition of the LC block (see Table 2). The block copolymer is microphase separated, but the order between domains is only short range. From the position of the reflection in the SAXS diagram, we determine the lattice constant of PSLC 97/3 based on the assumption of a cubic structure.

The recorded diffraction profiles were first desmeared[31] and then analyzed to determine the structure by fitting to a theoretical model. The method developed previously[32,33] describes the scattered intensity as a sum of three contributions: (i) Bragg reflections from the

Table 3. Mesophase Structure and Dimensions of the LC Block Obtained from the Fits: Thickness of the LC Layer in the Lamellar Mesophase, δ_{LC}, and Radius of the Spherical or Cylindrical LC Domains in the Hexagonal and Cubic Mesophases, R_{LC}

polymer	mesophase	structure	δ_{LC}, R_{LC} (nm)
PSLC 7/93	hexagonal	PS cylinders in LC matrix	
PSLC 14/86	hexagonal	PS cylinders in LC matrix	
PSLC 19/81	hexagonal	PS cylinders in LC matrix	
PSLC 30/70	hexagonal[a]	PS cylinders in LC matrix	
PSLC 39/61	lamellar	PS and LC lamellae	21.3
PSLC 59/41	lamellar	PS and LC lamellae	11.2
PSLC 77/23	lamellar	PS and LC lamellae	11.2
PSLC 85/15	hexagonal	LC cylinders in PS matrix	6.3
PSLC 97/3	cubic	LC spheres in PS matrix	4.7

[a] SAXS data are not well resolved.

domain structure modulated with the form factor of the scattering domains; (ii) diffuse scattering caused by the positional disorder and the size distribution of the microdomains; and (iii) background scattering from density fluctuations. The application of the fitting procedure results in information about the structure of the domains and determination of its characteristic length scales (i.e., lattice spacing and dimensions of the domains). In the cases of the lamellar mesophase, an analysis using the correlation function was performed,[29] which is directly calculated from the scattering pattern after subtraction of the flat background. This method results in both the period of the lamellar structure and the desired thickness of the LC layers (δ_{LC}). Table 3 summarizes the results obtained for the domain structure. In all cases, only one type of mesophase structure was obtained independent of the temperature. In other words, no order−order phase transitions were induced by the nematic/isotropic transition of the LC block. Such a transition was found recently for a triblock copolymer with the same mesogenic unit.[34] The domain structure persists over a broad temperature range, 25 up to 170 °C, and the disordered state was not reached even for the block copolymer with the lowest content of the LC block, PSLC 97/3. Obviously, the order-to-disorder temperature lies in a temperature range much higher than experimentally accessible.

The temperature dependence of the lattice spacing and the dimensions of the LC microdomains are presented in Figures 3 and 4, respectively. The average nematic/isotropic transition temperature is indicated by a dashed line. Figure 3 shows that in the broad temperature range from 25 to 170 °C, covering temperatures below as well as above the glass transitions of the PS and the LC block and the nematic/isotropic transition of the LC block, the lattice spacing is practically invariant for all block copolymers with the exceptions of PSLC 7/93 and PSLC 97/3. The lattice spacing for the PSLC 97/3 was determined with larger error (see Figure 3). For the sample with the large LC volume fraction, PSLC 7/93, we observe a marked decrease in the lattice spacing taking place in the vicinity of the nematic/isotropic transition of the LC block (Figure 3). Simultaneously, an increase of the radius of the PS spheres occurs (data not shown).[29] These two features indicate that in the vicinity of the nematic/isotropic transition of the LC block, the hexagonal structure becomes thermodynamically unstable and attempts to transform into an energetically preferred cubic structure. However, our efforts to fit the diffraction patterns obtained above the T_{ni} to a cubic mesophase structure

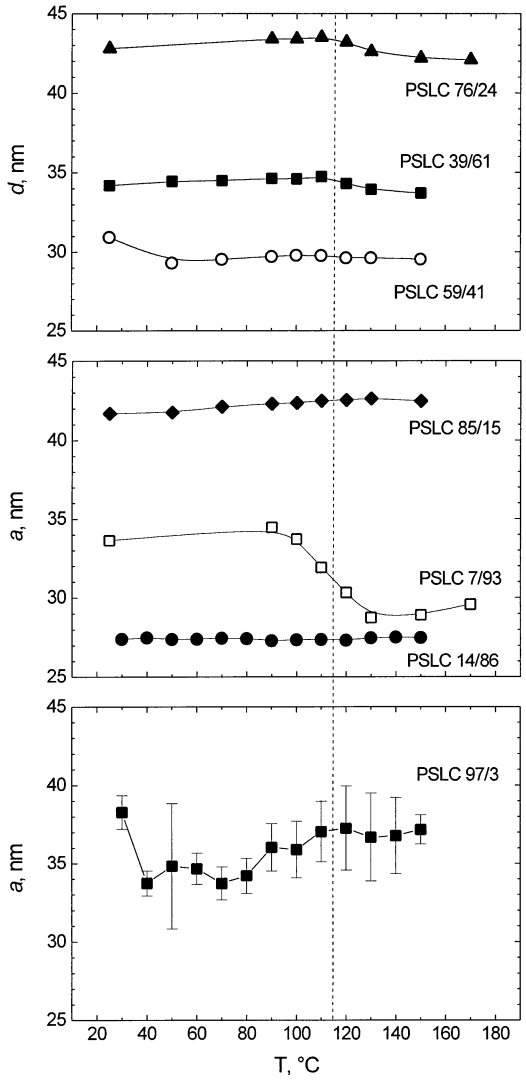

Figure 3. Dependence of lattice parameter on temperature: (top) *d* in lamellar mesophase; (middle) *a* in hexagonal mesophase; (bottom) *a* in cubic mesophase. Here and below error bars are drawn wherever they exceed the size of the symbols. The mean nematic/isotropic transition temperature is indicated by a dashed line.

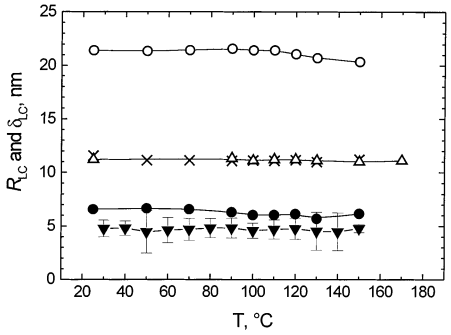

Figure 4. Temperature dependence of the dimensions of the LC domains (thickness of the LC layer, δ_{LC}, or radius of the cylinders or spheres, R_{LC}): (○) PSLC 39/61; (△) PSLC 59/41; (×) PSLC 76/24; (●) PSLC 85/15; (▼) PSLC 97/3.

were unsuccessful. The best fit remained the structure of hexagonally packed PS cylinders. For broader discussion, see ref 29.

An important issue for the present study is the variation of dimensions of the LC domains with temperature. Figure 4 shows explicitly that the dimensions

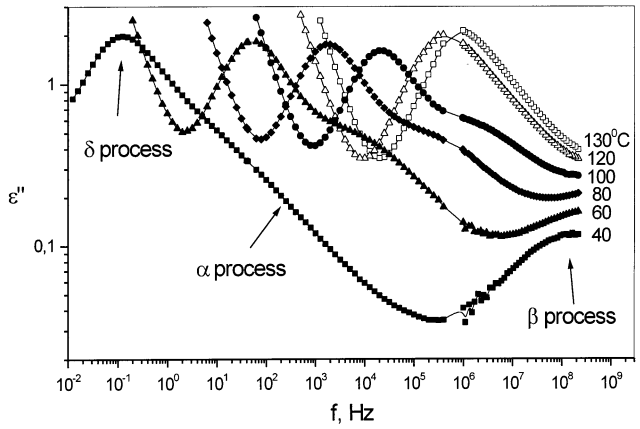

Figure 5. Dielectric spectra for the PSLC 0/100 at several temperatures as indicated in LC (solid symbols) and isotropic (open symbols) state.

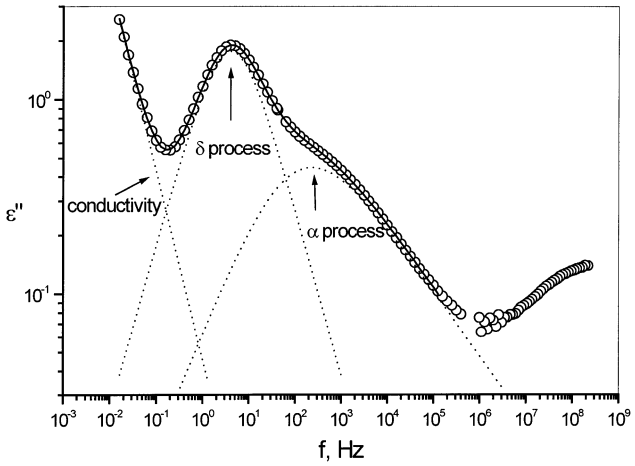

Figure 6. Example of the fitting results for the polymer PSLC 0/100 at 50.0 °C. The solid line is the sum of the three curves shown by the dashed lines: α relaxation ($\Delta\epsilon = 2.19 \pm 0.10$; $\alpha = 0.59 \pm 0.04$; $\gamma = 0.58 \pm 0.06$; $\tau = (1.71 \pm 0.12) \times 10^{-3}$s), δ relaxation ($\Delta\epsilon = 4.44 \pm 0.10$; $\alpha = 0.87 \pm 0.01$; $\gamma = 1.00$; $\tau = (4.24 \pm 0.05) \times 10^{-2}$s), and conductivity contribution ($\sigma/\epsilon_0 = 0.22 \pm 0.01$; $s = 0.92 \pm 0.01$).

of the LC domains are practically invariant in the temperature range from 25 to 170 °C. The values are summarized in Table 3.

3.2. Dielectric Spectroscopy. In the following, we present the results obtained from dielectric spectroscopy on the LC/I block copolymers. In the first section, we deal with the homopolymers and with those block copolymers for which the LC phase forms the continuous matrix. The second section then is devoted to the samples with the LC block confined in nanoscale domains.

3.2.1. General Features of the Dielectric Relaxation in the LC and PS Homopolymers and LC Matrix. Since in the investigated compositions each copolymer forms separate domains it is helpful to consider the individual dielectric behavior of the homopolymers involved: LC and PS. Figure 5 shows the dielectric spectra of the LC homopolymer in its nematic and its isotropic state. Two main relaxation processes denoted as δ and α are observed in the LC and isotropic states. In the isotropic state they overlap. This behavior is typical for the side chain LC polymers.[35,36]

Moreover it can be seen from Figure 5 that in the spectra at +40 °C an additional relaxation process appears at high frequencies. Its molecular origin is a local motion of the mesogen (β relaxation),[35,37] which we shall not consider in this paper.

To describe quantitatively the experimental spectra, the isothermal data of the dielectric losses ϵ'' were fitted to a superposition of two Havriliak−Negami (HN) functions[38] and a conductivity contribution appearing at low frequencies:

$$\epsilon^*(\omega) - \epsilon_\infty = \sum_k \frac{\Delta\epsilon_k}{(1 + (i\omega\tau_k)^{\alpha_k})^{\gamma_k}} - \frac{i\sigma}{\epsilon_0\omega^s} \qquad (1)$$

Here, ϵ_0 is the vacuum permittivity, $\Delta\epsilon_k$ the relaxation strength, and τ_k the relaxation time of the kth process. The shape parameters α_k and γ_k describe the symmetric and asymmetric broadening of the relaxation peak, respectively. For purely ohmic behavior σ denotes the dc conductivity and the exponent s equals 1. Values of s different from 1 are only used for a qualitative description of $\epsilon(\omega)$. In the case of $\alpha = \gamma = 1$, the HN function reduces to that of a Debye relaxation process. Special cases are the symmetric Cole−Cole function ($\alpha < 1$, $\gamma = 1$) or the asymmetric Cole−Davidson function

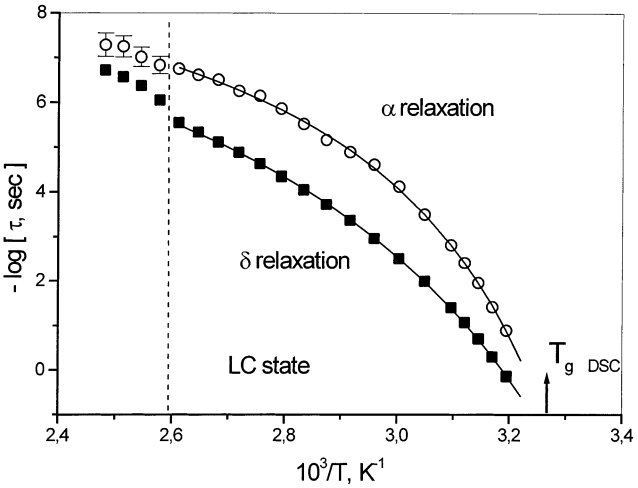

Figure 7. Relaxation time of both cooperative processes vs inverse temperature for the LC homopolymer. Lines are the fits of the VFT function to the data. The vertical dashed line marks the nematic/isotropic transition. The arrow indicates the glass transition temperature T_g as determined by DSC.

($\alpha = 1$, $\gamma < 1$). Equation 1 is fitted to the experimental data using a nonlinear least squares algorithm. The fit routine provides stable results for the relaxation times for the α and δ processes. The accuracies in the determination were generally better than 5% and 15%, respectively. Figure 6 shows an example of the fitting results for the LC homopolymer. It is seen that the δ and α relaxations are nicely separated using this procedure. Figure 7 displays the activation diagram for both relaxation processes. Both processes display a pronounced nonlinear temperature dependence of the relaxation time in Arrhenius coordinates (Figure 7). Therefore, for its description the phenomenological Vogel−Fulcher−Tammann (VFT) equation was used

$$\tau = A \exp\left(\frac{B}{T - T_v}\right) \qquad (2)$$

where τ is the relaxation time. A, B, and T_v are the VFT parameters. The constant A is the limiting value for the relaxation time at $T \rightarrow \infty$, T_v is the so-called Vogel

Table 4. VFT Parameters for α and *δ* Processes of the LC Block in Different Mesophases

	δ				α			
sample	$A \times 10^{10}$	B	T_v (K)	$T_{g,DIEL}$[a] (°C)	$A \times 10^{10}$	B	T_v (K)	$T_{g,DIEL}$[a] (°C)
				Homopolymer				
PSLC 0/100	0.82(±0.12)	1340(±30)	256(±1)	35	1.49(±0.50)	750(±30)	277(±1)	34
				LC Matrix				
PSLC 7/93	0.97(±0.25)	1320(±40)	257(±1)	36	3.20(±0.86)	680(±30)	279(±1)	34.0
PSLC 14/86	0.91(±0.25)	1340(±50)	257(±1)	37	2.75(±0.42)	680(±20)	279(±1)	34
PSLC 19/81	0.93(±0.18)	1340(±40)	257(±1)	37	3.55(±0.60)	670(±30)	281(±1)	34
PSLC 30/70	0.87(±0.25)	1340(±50)	257(±1)	37	5.63(±1.5)	630(±30)	281(±1)	35
				Lamellar Structure (LC Thin Films, 1D Confined)				
PSLC 39/61	0.56(±0.21)	1390(±60)	256(±2)	37	1.25(±0.42)	770(±30)	276(±1)	34
PSLC 59/41	1.91(±1.02)	1600(±90)	249(±2)	36	0.82(±0.17)	840(±30)	273(±1)	32
PSLC 77/23	4.86(±1.20)	1460(±70)	252(±2)	35	1.70(±0.56)	750(±40)	275(±2)	32
				Cylindrical Structure (LC Microdomain, 2D Confined)				
PSLC 85/15	2.88(±2.03)	1600(±100)	245(±3)	32	1.16(±0.47)	790(±50)	271(±2)	29

[a] Determined from eq 2 at $\tau = 10$ s.

temperature which is usually found to be 30−50 °C lower than T_g, and B is an activation parameter. The calculated VFT parameters are presented in Table 4. The glass transition temperature ($T_{g,DIEL}$) was determined at $\tau = 10$ s.

Concerning the microscopic dynamics underlying the *δ* and α processes in side chain LC polymers there appears to be no unique picture at present. Various models have been proposed.[35,37,39,40] The most extensively discussed model for the low frequency *δ* relaxation assumes that it is caused by cooperative rotation of the side groups. The large relaxation strength and its dependence on the longitudinal component of the side groups dipole moment confirm this model. The *δ* relaxation has a narrow and symmetrical absorption curve. Therefore, we have used the symmetrical HN (i.e., Cole−Cole) function for this relaxation in the fit routine described above (eq 1). We thus reduce the number of variable parameters in the fitting process and hence increase fit stability. In contrast to the *δ* process, the high-frequency α relaxation is characterized by a very broad and asymmetrical regime of dielectric absorption. The results of this analysis are the relaxation times τ for both processes in a wide range of temperatures. We display these data in Figure 7. The temperature dependence of the α relaxation is strongly nonlinear in the Arrhenius coordinates. This is a characteristic feature of the dynamic glass transition in amorphous polymers. In most cases, the appearance of this process coincides with the calorimetric glass transition temperature of the polymer, which is also a formal basis for referring it to a segmental motion. TSDC experiments also confirm this assignment especially for LC polymers containing a cyanobiphenyl mesogenic fragment,[41−43] i.e., systems similar to those investigated in the present work.

It is interesting to observe that α and *δ* relaxations are dynamically coupled.[44] Their temperature variation is governed by nearly the same T_g.[45] (see Table 4).

The dielectric properties of bulk PS homopolymers are well described in the literature.[46] We therefore only briefly comment on its dielectric relaxation. PS displays a typical α relaxation with very small relaxation strength. The maximum value for the loss part of the dielectric function is $\epsilon''_{max} \leq 0.01$. In comparison to that, the intensities of the dielectric processes related to the LC block are much stronger. Depending on volume fraction of LC block the ϵ''_{max} varies between 2 and 0.1. The α relaxation of the PS block is therefore hardly discernible in the spectra.

We now turn to the block copolymers with a PS volume fraction up to 30%. The SAXS study of samples PSLC 7/93, PSLC 14/86, PSLC 19/81, and PSLC 30/70 has shown that they may be considered as a continuous LC matrix with embedded PS cylinders. The LC blocks of these copolymers reveal a dielectric relaxation pattern which is quite similar to that of the LC homopolymer. However, the frequency position of the *δ* and α peaks is slightly shifted to lower values. This means that both cooperative modes of the LC block become slower in the block copolymer matrix, i.e., the glass transition temperature $T_{g,DIEL}$ is increased. The origin of this shift lies in the strongly segregated structure of the block copolymers and will be discussed in a subsequent section. The VFT parameters for both cooperative modes and the calculated $T_{g,DIEL}$ values are summarized in the Table 4.

3.2.2. Dielectric Behavior of Nanoscale Confined LC Blocks. In the compositions PSLC 39/61, PSLC 59/41, and PSLC 77/23, the LC blocks form layers of thickness 21, 11, and 11 nm, respectively. We call this a 1D confinement, which could be also considered as an analogue of the thin film. For PSLC 85/15 the LC blocks are confined in cylindrical domains with diameter of 12 nm (2D confinement), which are embedded in a continuous PS matrix. A common feature found for these compositions is the appearance of a new relaxation peak in the dielectric spectra. At low frequencies in addition to the *δ* and α processes we find a strong relaxation regime. As an example, Figure 8 displays the dielectric spectra for PSLC 59/41 recorded in the temperature range around the nematic/isotropic transition.

The analysis of these data is done as described above. The results are summarized in Table 4 and Figure 9. It is clearly seen from Figure 9 that the relaxation time for the additional slow process is by ∼4 orders of magnitude larger than the relaxation times of the cooperative processes. We have assigned this process to the interfacial Maxwell−Wagner (MW) polarization which is usually developed in heterogeneous systems.[47] For the composition PSLC 39/61 we were unable to extract clearly this relaxation due to a high conductivity of the sample.

The relaxation time of the MW relaxation may be calculated on the basis of the dielectric properties, the conductivity, the domain form and size. According to van Beek's calculations for the simplest model of a medium consisting of two different layers the MW relaxation time can be written as[47]

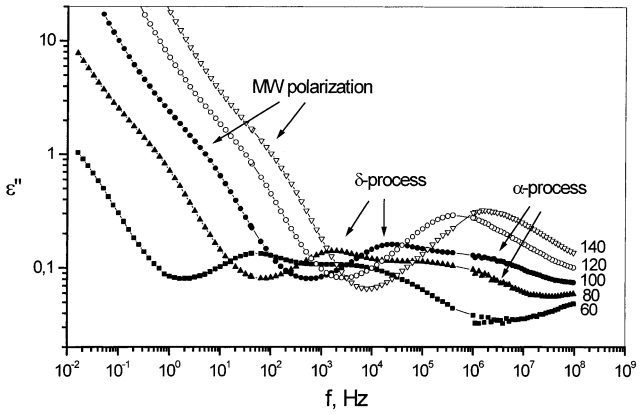

Figure 8. Dielectric spectra for the PSLC 59/41 at different temperatures: in LC (solid symbols) and isotropic (open symbols) states.

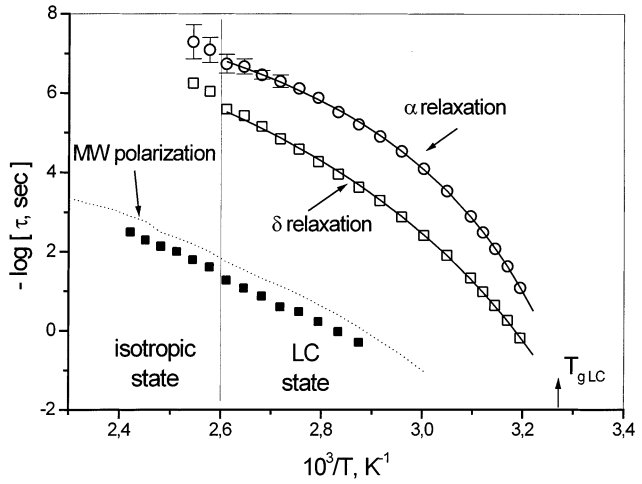

Figure 9. Relaxation time of cooperative and MW processes vs inverse temperature for the sample PSLC 59/41. The dashed line was calculated according to eq 3. The vertical line denotes the nematic/isotropic transition inside the LC microdomains.

$$\tau_{MW} = \frac{\epsilon'_1(T)d_2(T) + \epsilon'_2(T)d_1(T)}{\sigma_1(T)d_2(T) + \sigma_2(T)d_1(T)} \quad (3)$$

where $d_1$and d_2 are the thicknesses for layers 1 and 2 with permittivities ϵ'_1 and ϵ'_2 and conductivities σ_1 and σ_2, respectively. We can directly apply this relation for the composition PSLC 59/41 and PSLC 77/23 forming lamellar structures. In our calculations we used data published earlier for PS ($\epsilon'_1(T)$, $\sigma_1(T)$)[46] and our own results for LC homopolymer ($\epsilon'_2(T)$ and $\sigma_2(T)$) and data for layer thickness ($d_1(T)$ and $d_2(T)$). The values thus calculated at each temperature for PSLC 59/41 are also shown by the dotted line in Figure 9. This line deviates slightly from the experimental data. Such deviation between theoretical and experimental values may be caused by the uncertainty in the determination of the conductivity of the PS (σ_1) and LC (σ_2) layers in the copolymers.

It is important to note that the samples discussed here, especially PSLC 85/15 reveal a faster cooperative motion near the glass transition in comparison to the LC matrix, i.e., the glass transition temperature $T_{g,DIEL}$ is decreased (see Table 4). This effect will be considered in the next section.

With regard to the PSLC 97/3 sample, we note that the α and δ relaxations cannot be seen as clearly resolved processes. A very broad relaxation regime is observed, which cannot be separated into both processes. PSLC 97/3 is consequently left out of part of the subsequent discussion.

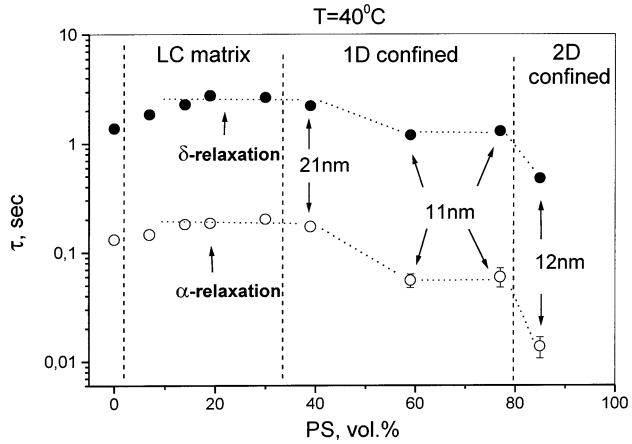

Figure 10. Relaxation time of the cooperative processes of LC block at 40 °C as a function of PS volume fraction. The vertical dashed lines separate approximately the different mesophase structures (see Table 3).

3.3. Discussion. The dielectric relaxation in the LC/I diblock copolymers is mainly due to the contribution from the LC block. We may therefore use these systems to investigate the effect of confinement on the molecular dynamics of the LC copolymer. In this view we consider the LC homopolymer (PSLC 0/100) as a bulk or nonconfined system. The samples PSLC 7/93, PSLC 14/86, PSLC 19/81, and PSLC 30/70 consist of a LC matrix with embedded PS domains and therefore form a nonconfined system too. The PSLC 39/61, PSLC 59/41, and PSLC 77/23 are alternate layers of LC and PS and therefore termed 1D-confined systems. The LC layer thicknesses are 21, 11, and 11 nm, respectively. In PSLC 85/15 the LC blocks are contained in the cylindrical domains with diameter of 12 nm. It may be considered as a 2D confinement. We recall that we have assigned the α process to a segmental motion of the main chain. The δ process is due to the rotation of the side group as a whole. However, these two processes are dynamically coupled. The frequency−temperature location of both processes in an Arrhenius plot is determined basically by the α process, i.e., by the main chain rigidity of LC macromolecule. This idea explains the partial parallelism of the temperature and the pressure dependencies of the α and δ processes within the mesomorphic state.[36] Recently we have shown that the gradual increase on the backbone rigidity of the functionalized LC copolymer caused the parallel slow of the reorientation rates of both processes.[44] In other words, the change of the backbone rigidity of LC side chain polymer (α process) will cause a corresponding variation of the δ process. In the present work, we find that the relaxation times of the α and δ processes are related by a factor which does not change for different mesostructures although the absolute values of relaxation times can vary considerably. This is clearly seen in Figure 10 where we show the relaxation time of cooperative processes at 40 °C vs the PS volume fraction, i.e., as a function of different states of LC blocks: from bulk via matrix with PS inclusions to nanoconfined states in PS matrix. The relaxation times of both processes vary jointly over the range of composition studied.

A further observation from Figure 10 is that the relaxation time of both cooperative modes for the LC block becomes slightly slower (factor of 2) when moving from the LC homopolymer into the matrix situation. This slowing down is caused by the block copolymer structure of the molecule. One end of the LC main chain is connected to the PS block via a covalent bond and therefore located at the PS domain. Bulk PS has a T_g at about 100 °C and below this temperature its segmental dynamics is completely frozen. As a result the segmental dynamics of the tethered LC chains with T_g at about 35 °C will also be partly suppressed. This gives rise to a slowdown of the α process and consequently changes the δ process due to the strong dynamical coupling between both. There have been several comparative studies of the segmental motion in homopolymers and their diblock copolymers in the microphase separated state. For the polyisoprene and polystyrene−polyisoprene[48] and poly(oxybutylene) and poly(oxyethylene)−poly(oxybutylene)[49] it has been shown that the retardation factor is of the order of 2−4 in a broad range of composition (volume fraction 0.16−0.65). A similar magnitude of retardation of the segmental mode is obtained for the LC matrix samples studied in the present work: PSLC 14/86, PSLC 19/81, and PSLC 30/70 (see Figure 10).

Moving to larger volume fraction of PS, for which the LC blocks are confined to layers of thickness of 21 nm (PSLC 39/61), the relaxation times are the same as in the LC matrix. As the confinement length decreases further to 11 nm (PSLC 59/41 and PSLC 76/24), the relaxation time even becomes significantly shorter. The effect is most pronounced for PSLC 85/15, which exhibits 2D confinement. The overall change in relaxation time is in the range of 1 order of magnitude for each cooperative mode. This observation is in a qualitative agreement with results of the cooperative dynamics near the glass transition in restricted geometries for the low molecular weight glass-forming liquids[2−4,6−9] and in thin polymer films.[13−23]

Using dielectric spectroscopy, it was shown recently for thin films of PS that the relaxation time of the segmental mode remains constant down to a critical thickness d_c.[23] Below d_c, the relaxation times decrease drastically with decreasing thickness. A further important finding of the above work is that the d_c values display a molecular weight dependence and are apparently related to the radius of gyration of polymer chains (for PS $d_c = 11$ nm for $M_W = 2{,}8 \times 10^5$ and $d_c = 22$ nm for $M_W = 1{,}8 \times 10^6$). In compositions PSLC 39/61, PSLC 59/41, and PSLC 77/23, the LC block has a similar degree of polymerization (DP ∼ 50) and hence we can estimate d_c to be between 21 and 11 nm.

As was already mentioned above the temperature variation of the α process is controlled by the dynamic glass transition of the LC copolymer. The corresponding $T_{g,DIEL}$ values are presented in Table 4. The difference between $T_{g,DIEL}$ for bulk and 12 nm 2D-confined samples is only 5 °C. For comparison, the directly measured T_g values for the PS thin films on substrate were lower than the bulk values for films with thickness less that 40 nm.[13] The total T_g reduction for a film of thickness 20 nm was ∼10 °C, whereas the freely standing PS film with the same thickness exhibited ∼70 °C reduction of T_g.[14] These measurements demonstrate the strong effect of the free surface on T_g of thin polymer films. On the basis of these results the T_g reduction was discussed in the context of a two- or three-layer model[17,18,21,23,50] in which the thin film was suggested to consist of two or three layers with different mobility and corresponding glass transition temperatures. These models suggested that near a free surface interface there exists a "liquidlike" layer, in which the molecular mobility is much higher than in bulk. Close to the substrate−polymer interface a so-called "bound" or "dead" layer is formed, where the mobility is considerably suppressed. In addition to this the three-layer model assumes the existence of the "bulklike" phase between "liquidlike" and "dead" layers.

It should be noted that the LC blocks studied in this work have two symmetrical interfaces LC−PS with strong coupling between them. One end of the LC main chain is connected to PS domain via a covalent bond. Although these tethered LC molecules would be expected to have a lower mobility, we still found T_g decreasing. However, the range of these changes is weak in comparison with data on PS thin films on substrate.[13]

In addition to the confinement effect we have to consider two other factors, which may affect the segmental dynamics of the LC block. First of all a molecular weight dependence of cooperative modes should be taken into account, since the investigated copolymers have the different LC main chain length. According to literature data, the maximum rise in the relaxation time of both cooperative modes of side chain LC polymers with increasing molecular weight is observed at a degree of polymerization up to 30−40.[51] At higher DP values, the cooperative dynamics is virtually independent of the main chain length. Our copolymers have a DP of LC block between 50 and 200. The difference in molecular weight of our copolymers therefore cannot cause any significant changes in the parameters of both cooperative modes.

Another factor we may have to consider is the influence of nematic director orientation with respect to the external field on the dielectric relaxation. Within the LC domains, the mesogens have a preferred orientation in the plane.[52,53] The lamellar domains themselves show no preferred orientation in the bulk sample and consequently the nematic director is not oriented. To check the possible variation of the dielectric relaxation with director orientation we have prepared homeotropically and planar aligned samples of the LC homopolymer PSLC 0/100 by applying an alternating high voltage electrical field to the sample. In the method of sample orientation, we generally followed to the strategy reported in ref 40. A detailed account of these results will be presented in a separate paper. For the present discussion, it is important to note that the frequency−temperature locations and the shapes of both cooperative modes are practically independent of the type and the degree of alignment developed in the homopolymer as well as in the copolymers. This is in agreement with data published earlier on an oriented LC side chain polymer containing a similar mesogen fragment.[40]

We now turn to the shape of the dielectric function, which is controlled by the distribution of relaxation times. Without specification of a model, the shape of the dielectric loss function near a peak at $\omega = \omega_{max}$ is characterized by two limiting parameters, m and n:

$$\epsilon''(\omega) \propto \omega^m \quad (\omega \ll \omega_{max})$$

$$\epsilon''(\omega) \propto \omega^{-n} \quad (\omega \gg \omega_{max})$$

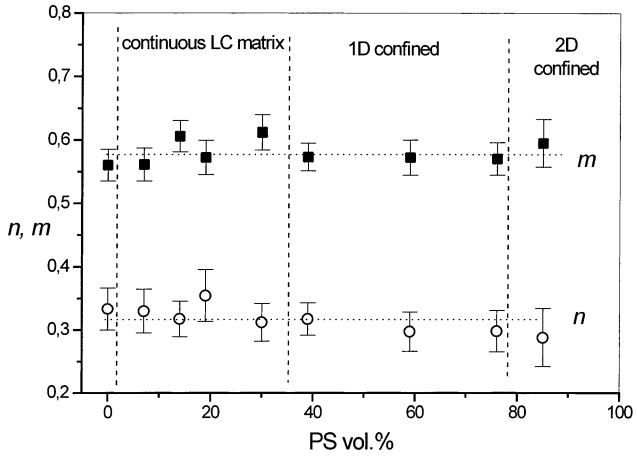

Figure 11. α relaxation shape parameters *m* and *n* at 40 °C for different compositions. The vertical dashed lines separate approximately the different mesophase structures (see Table 3).

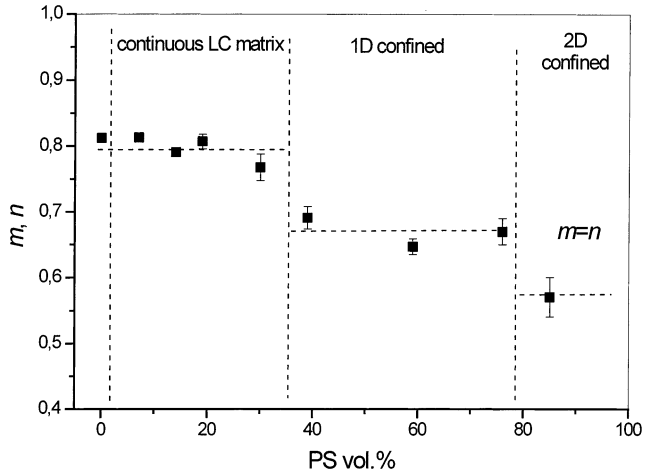

Figure 12. δ relaxation shape parameters *m* and *n* at 40 °C for different composition. The vertical dash lines separate approximately the different mesophase structures (see Table 3).

They are related to the HN parameters in eq 1 by $m = \alpha_{HN}$ and $n = (\alpha_{HN}\gamma_{HN})$. These two parameters are of particular interest since they are affected by long- (low frequency) and short-range (high frequency) motion correlation.[54,55] There are contradicting observations on the influence of spatial confinement on the shape parameters. It was documented in many dielectric studies that the α process becomes broader in the confined state.[1−9,21−23] The broadening is interpreted as being caused by relatively immobile molecules close to a pore wall[1−9] or to the substrate.[21−23] A test of this idea was performed by special chemical treatment of the pore wall with the intent to decouple the molecules from the solid wall. It was found that the distribution of relaxation times slightly narrowed.[3,9] The interaction between the molecule and the pore wall cannot be removed completely. A similar situation is encountered for diblock copolymers in their microphase separated state. The segmental mode itself does not reveal any significant broadening in comparison to the homopolymer.[48,49] A broadening is found, however, for the normal mode of polyisoprene in block copolymers with polystyrene as a consequence of the fixing of one end of the PI chain to the PS domain in the ordered state.[27] This mode is particularly sensitive to the end-to-end relaxation of the PI block. By means of photon correlation spectroscopy on freely standing PS films, it was found that the distribution of relaxation times of segmental mode for a film of thickness of ∼25 nm was indistinguishable from that of bulk PS.[56] At the same time Tg was reduced by 70 °C compared to the bulk value. Recent dielectric investigation of *cis*-polyisoprene thin films (down up to 22 nm) reveal that segmental relaxation as well as the shape of relaxation peak are unaffected by confinement.[20] These results suggest that the dynamics on microscopic level are not affected by confinement down to ∼20 nm and that the relevant length scale is much larger than the cooperativity length for segmental motion. The values of the shape parameters *m* and *n* at 40 °C for the α relaxation are plotted in Figure 11. They were obtained from a fit of eq 1 to the data. Both parameters have values that are typical for the segmental mode of amorphous polymers[38] and do not vary within the experimental uncertainty over the range of composition studied. The latter fact implies that the distribution of relaxation times for segmental mode is the same in the bulk and nanoconfined samples. This leads us to the same conclusion concerning the segmental motion of LC blocks and its length scale of cooperativity as established in the above work on freely standing PS films.[56]

In contrast to the α relaxation, the shape parameters of the δ process reveal a decrease on reducing the confinement length. This can be seen in Figure 12 in which we show the *m* and *n* parameters at 40 °C for the δ relaxation in all copolymers studied. As we kept the γ parameter for that process always equal to 1 in the fit routine by eq 1, this implies that $m = n$ and the symmetrical distribution of relaxation time. We have assigned the δ process to the side chain reorientation as a whole. The cooperativity length for this relaxation is obviously larger than that of the segmental motion. It was found recently that the relaxation time of the δ process jumps discontinuously at the S_E to S_A transition in LC dendrimers.[57] It may therefore be expected to be more sensitive to confinement and hence show a broadening of the relaxation peak.

Conclusion

We have investigated a series of isotropic/liquid crystalline diblock copolymers with narrow molecular weight distribution and with well-defined chemical structure. The volume fraction of both blocks is varied and covers the full range of composition. As a result of the strong incompatibility between the PS block and the LC block the polymers were found to be microphase separated in the full temperature regime from 25 up to 170 °C. The SAXS pattern allowed the determination of domain structure and size. In contrast to an earlier study of a triblock copolymer,[34] we do not find a clear order-to-order transition for these samples although the LC domains undergo a nematic to isotropic transition. This was found to trigger a change in domain form from cylindrical to spherical domains for the triblock copolymer. The coupling between domain form and LC order is seen in the disturbance of the nematic field of the LC matrix by the inclusions. For the present series of diblocks the correlation between orientational order in the LC and the domain form is apparently weaker. Only a variation of the domain size is observed when approaching the phase transition.

The variation of volume fraction in the diblock copolymers allows us to study the molecular dynamics

for different and well-defined spatial constraints. The homopolymer represents a continuous undisturbed matrix. Increase of the PS content results in a matrix with cylindrical inclusions and to systems of alternating layers of PS and LC. Finally the LC is contained in domains of cylindrical or spherical form. The dynamics is studied here with dielectric spectroscopy, which monitors the α and δ relaxation. They are related to the segmental motion of main chain and mesogen and the relaxation of the mesogen as a whole, respectively. For all samples we find a joint variation of both relaxations with temperature. They are both controlled by the glass transition of the LC phase. The influence of spatial constraint is seen in the absolute value of the relaxation times. Whereas the coupling of the LC block to the PS domain primarily has the effect of an increase in the relaxation time, we find the opposite behavior at a larger PS fraction, i.e., stronger spatial constraint. The relaxation times of both α and δ relaxations are significantly decreased. This points into the same direction as the observations made on thin films of polymers. However, the block copolymer represents a physically different system with the boundary layer between the domains defined by the chemical bond and the thermodynamics of mixing between both components. As we have seen no strong change in the width of the relaxation regime of the α relaxation, we can exclude a strong heterogeneity of the segmental dynamics. Only the δ process broadens with increasing confinement. The molecular dynamics underlying the α and δ relaxations are apparently governed by different characteristic lengths. The picture of layers with variable mobility proposed in several studies[17,18,23,50] does not seem appropriate for the present situation. The influence of spatial constraints on the dynamics may be through a modification of the local orientational order.

References and Notes

(1) Schüller, J.; Melnichenko, Y. B.; Richert, R.; Fischer, E. W. *Phys. Rev. Lett.* **1994**, *73*, 2224−2227.
(2) Schüller, J.; Richert, R.; Fischer, E. W. *Phys. Rev. B* **1995**, *52*, 15232−15238.
(3) Gorbatschow, W.; Arndt, M.; Stannarius, R.; Kremer, F. *Europhys. Lett.* **1996**, *35*, 719−724.
(4) Huwe, A.; Kremer, F.; Behrens, P.; Schwieger, W. *Phys. Rev. Lett.* **1999**, *82*, 2338−2341.
(5) Huwe, A.; Arndt, M.; Kremer, F.; Haggenmüller, C.; Behrens, P. *J. Chem. Phys.* **1997**, *107*, 9699−9701.
(6) Arndt, M.; Stannarius, R.; Groothues, H.; Hempel, E.; Kremer, F. *Phys. Rev. Lett.* **1997**, *79*, 2077−2080.
(7) Pissis, P.; Kyritsis, A.; Daoukaki, D.; Barut, G.; Pelster, R.; Nimtz, G. *J. Phys.: Condens. Matter* **1998**, *10*, 6205−6227.
(8) Daoukaki, D.; Barut, G.; Pelster, R.; Nimtz, G.; Kyritsis, A. G.; Pissis, P. *Phys. Rev. B* **1998**, *58*, 5336−5345.
(9) Kremer, F.; Huwe, A.; Arndt, M.; Behrens, P.; Schwieger, W. *J. Phys.: Condens. Matter* **1999**, *11*, A175-A188.
(10) Wendt, H.; Richert, R. *J. Phys.: Condens. Matter* **1999**, *11*, A199-A206.
(11) Park, J.-Y.; McKenna, G. B. *Phys. Rev. B* **2000**, *52*, 6667−6676.
(12) Petychakis, L.; Floudas, G.; Fleischer, G. *Europhys. Lett.* **1997**, *40*, 685−690.
(13) Keddie, J. L.; Jones, R. A. L.; Cory, R. A. *Europhys. Lett.* **1994**, *27*, 59−64.
(14) Forrest, J. A.; Dalnoki-Veress, K.; Stevens, J. R.; Dutcher, J. R. *Phys. Rev. Lett.* **1996**, *77*, 2002−2005.
(15) Forrest, J. A.; Dalnoki-Veress, K.; Stevens, J. R.; Dutcher, J. R. *Phys. Rev. E* **1997**, *56*, 5705−5716.
(16) Forrest, J. A.; Dalnoki-Veress, K.; Stevens, J. R.; Dutcher, J. R. *Phys. Rev. E* **1998**, *58*, 6109−6114.
(17) Mattsson, J.; Forrest, J. A.; Börjesson, L. *Phys. Rev. E* **2000**, *62*, 5187−5200.
(18) Tseng, K. C.; Turro, N. J.; Durning, C. J. *Phys. Rev. E* **2000**, *61*, 1800−1811.
(19) Grohens, Y.; Sacristan, J.; Hamon, L.; Reinecke, H.; Mijangos, C.; Guenet, J. M. *Polymer* **2001**, *42*, 6419−6423.
(20) Jeon, S.; Granick, S. *Macromolecules* **2001**, *34*, 8490−8495.
(21) Kremer, F.; Hartmann, L. *Dielectr. Newsl.* **2001**, *Sept*, 4−6.
(22) Fukao, K.; Miyamoto, Y. *Europhys. Lett.* **1999**, *46*, 649−654.
(23) Fukao, K.; Miyamoto, Y. *Phys. Rev. E* **2000**, *61*, 1743−1754.
(24) Floudas, G.; Paraskeva, S.; Hadjichristidis, N.; Fytas, G.; Chu, B.; Semenov, A. N. *J. Chem. Phys.* **1997**, *107*, 5502−5509.
(25) Floudas, G.; Hadjichristidis, N.; Iatrou, H.; Pakula, T. *Macromolecules* **1996**, *29*, 3139−3146.
(26) Floudas, G.; Meramveliotaki, K.; Hadjichristidis, N. *Macromolecules* **1999**, *32*, 7496−7503.
(27) Stühn, B.; Stickel, F. *Macromolecules* **1992**, *25*, 5306−5312.
(28) Sänger, J.; Gronski, W. *Macromol. Chem. Phys.* **1998**, *199*, 555−561.
(29) Ivanova, R.; Staneva, R.; Geppert, S.; Heck, B.; Walter, B.; Gronski, W.; Stühn, B. Manuscript in preparation.
(30) Matsen, M. W.; Bates, F. S. *Macromolecules* **1996**, *29*, 1091−1098.
(31) Strobl, G. *Acta Crystallogr.* **1970**, *A26*, 367−375.
(32) Heck, B.; Arends, P.; Ganter, M.; Kressler, J.; Stühn, B. *Macromolecules* **1997**, *30*, 4559−4566.
(33) Schwab, M.; Stühn, B. *Colloid Polym. Sci.* **1997**, *275*, 341−351.
(34) Sänger, J.; Gronski, W.; Maas, S.; Stühn, B.; Heck, B. *Macromolecules* **1997**, *30*, 6783−6787.
(35) Zentel, R.; Strobl, G.; Ringsdorf, H. *Macromolecules* **1985**, *18*, 960.
(36) Moscicki, J. K. Dielectric relaxation in macromolecular liquid crystals. In *Liquid crystal polymers−from structures to applications*; Collyer, A. A.; Ed.; Elsevier: Amsterdam, The Netherlands, 1992.
(37) Gedde, U. W.; Liu, F.; Hult, A.; Sahlen, F.; Boyd, H. *Polymer* **1994**, *35*, 2056−2062.
(38) Havriliak, S.; Hegami, S. *J. Polym. Sci., Part C* **1966**, *14*, 99.
(39) Haase, W.; Bormuth, F. J.; Pfeiffer, M.; Jakob, E. *Ber. Bunsen-Ges. Phys. Chem.* **1991**, *95*, 1050−1054.
(40) Attard, G.; Williams, G. *Liq. Cryst.* **1986**, *1*, 253−269.
(41) Mano, F. J.; Correia, N. T.; Ramos, J. M. *Polymer* **1994**, *35*, 3561−3564.
(42) Mano, F. J.; Ramos, J. M.; Fernandes, A.; Williams, G. *Polymer* **1994**, *35*, 5170−5178.
(43) Mano, F. J.; Correia, N. T.; Williams, G. *Liq. Cryst.* **1996**, *20*, 201−218.
(44) Zhukov, S.; Stühn, B.; Borisova, T.; Barmatov, E.; Barmatova, M.; Shibaev, V.; Kremer, F.; Pissis, P. *Macromolecules* **2001**, *34*, 3615−3625.
(45) Schönhals, A.; Wolff, D.; Springer. J. *Macromolecules* **1998**, *31*, 9019−9025.
(46) Rerrier, G.; Bergeret, A. *J. Appl. Phys.* **1995**, *77*, 2651−2658.
(47) Van Beek, L. K. H. Dielectric behaviour of heterogeneous systems. In *Progress in Dielectrics*; Birks, J. B., Ed.; Heywood: London, 1967; Vol. 7, pp 69−114.
(48) Yao, M.-L.; Wanatabe, H.; Adachi, K.; Kotaka, T. *Macromolecules* **1991**, *24*, 2955−2962.
(49) Kyritsis, A.; Pissis, P.; Mai, S.-M.; Booth, C. *Macromolecules* **2000**, *33*, 4581−4595.
(50) DeMaggio, G. B.; Frieze, W. E.; Gidley, D. W.; Zhu, M.; Hristov, H. A.; Yee, A. F. *Phys. Rev. Lett.* **1997**, *78*, 1524−1527.
(51) Novotna, E.; Kostromin. S.; Kresse, H. *Liq. Cryst.* **1995**, *18*, 73−80.
(52) Figueiredo, P.; Geppert, S.; Brangsch, R.; Bar, G.; Thomann, R.; Spontak, R. J.; Gronski, W.; Samlenski, R.; Müller-Buschbaum, P. *Macromolecules* **2001**, *34*, 171−180.
(53) Osuji, C. O.; Chen, J. T.; Ober, C. K.; Thomas, E. L. *Polymer* **2000**, *41*, 8897−8907.
(54) Schönhals, A.; Schlosser, E. *Colloid Polym. Sci.* **1989**, *267*, 125−132.
(55) Schiener, B.; Böhmer, B.; Loidl, A.; Chamberlin, R. V. *Science* **1996**, *274*, 752−754.
(56) Forrest, J. A.; Svanberg, C.; Revesz, K.; Rodahl, M.; Torell, L. M.; Kasemo, B. *Phys. Rev. E* **1998**, *58*, R1226−R1229.
(57) Trahasch, B.; Frey, H.; Lorenz, K.; Stühn, B. *Colloid Polym. Sci.* **1999**, *277*, 1186−1192.

MA020509+